

Stable optical spring in the Advanced LIGO detector with unbalanced arms and in the Michelson-Sagnac interferometer

Nikita Vostrosablin* and Sergey P. Vyatchanin

Physics Department, Moscow State University, Moscow 119992, Russia

(Received 2 January 2014; published 24 March 2014)

Optical rigidity in the Advanced LIGO gravitational-wave detector, operated on the dark port regime, is unstable. We show that the same interferometer with excluded symmetric mechanical mode but with unbalanced arms allows us to get stable optical spring for the antisymmetric mechanical mode. The arm detuning necessary to get stability is shown to be a small one—it corresponds to small power in the signal port. We show that stable optical spring may be also obtained in the Michelson-Sagnac interferometer with both power and signal recycling mirrors and unbalanced arms.

DOI: [10.1103/PhysRevD.89.062005](https://doi.org/10.1103/PhysRevD.89.062005)

PACS numbers: 04.80.Nn

I. INTRODUCTION

Ground-based gravitational wave antennas form a worldwide net of large-scale detectors like LIGO [1,2], VIRGO [3], and GEO [4]. The extremely high sensitivity of these detectors is limited by noises of different nature. In the low-frequency range (around 10 Hz) the gravity-gradient (Newtonian) noise prevails, below ~ 50 Hz—seismic ones, at middle frequencies ($\sim 50 - 200$ Hz) thermal noises dominate, and in the high-frequency range (over 200 Hz) photon shot noise makes the main contribution. The next generation of gravitational wave antennas (Advanced LIGO or aLIGO [2], Advanced VIRGO [5]) and also third-generation detectors (such as the Einstein Telescope [6,7], GEO-HF [8], and KAGRA [9]) promise by compensation and suppression of thermal and other noises to achieve sensitivity of standard quantum limit (SQL) [10–13] for continuous eigen measurement defined only by quantum noise. SQL is the optimal combination of two noises of quantum nature: fluctuations of light pressure caused by random photon number falling onto the mirror's surface and photon counting noise.

A possible way to overcome the SQL is the usage of optical rigidity (optical spring effect) [13–16]. Recall that optical rigidity appears in a detuned Fabry-Perot interferometer—the circulating power and consequently the radiation pressure became dependent on the distance between the mirrors. It has been shown [17–24] that gravitational wave detectors using optical springs exhibit sensitivity below the SQL.

In the case of a single pump an interferometer utilizing optical rigidity has two subsystems: a mechanical one and an optical one. Interaction between them gives birth to two eigenmodes, each of which is characterized by its own resonance frequency and damping. For a description of evolution one can make transfer from the conventional

coordinates to eigen ones and consider the evolution of the system as evolution of these (normal) oscillators [25].

The dynamics of a complex system such as the aLIGO detector can be considered on the basis of a simpler and better studied system—the Fabry-Pero resonator. Such equivalence is termed the “scaling law” [26]. The Fabry-Pero resonator with only one optical spring is always unstable because a single pump introduces either positive spring with negative damping or negative spring with positive damping [14–17]. The obvious way to avoid instabilities is by implementation of feedback [20]. Another way is utilization of additional pump [27,28], which has been investigated in detail and proven experimentally with a mirror of gram scale [29].

DC readout, planned in aLIGO, means the introduction of small detuning of arm length. Recall that the Michelson interferometer with balanced Fabry-Perot (FP) cavities in arms with power and signal recycling mirrors (aLIGO configuration, see Fig. 1) operating in the dark port regime

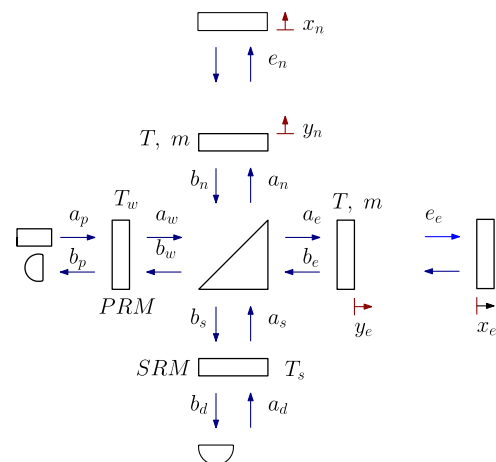


FIG. 1 (color online). Scheme of Advanced LIGO detector. PRM (SRM) are power (signal) recycling mirrors.

*vostrosablin@physics.msu.ru

possesses symmetric and antisymmetric modes, laser pump symmetric mode, and no mean intensity appears in the signal (dark) port through the signal recycling mirror (SRM). In the case of slightly detuned arms, small mean intensity appears in the signal port. This intensity is used as a very stable local oscillator.

The natural question is what arbitrary (not small) detuning in the arms may give stability. This question became interesting especially after the paper of Tarabrin *et al.* [30] demonstrated the possibility of stable optical spring in the Michelson-Sagnac interferometer with movable membrane [31–33]. The analyzed interferometer with the signal recycling mirror (SRM) but without the power recycling (PRM) was pumped through the power port [30]—a similar configuration is shown in Fig. 2 (but with PRM). However, stability of the optical spring was shown for relatively large detuning, which means relatively large power in the signal port, which is not convenient in experiment. Operation far from the dark port regime additionally creates the problem of laser noises leaking into the signal port, which makes it difficult to apply these results to the GW detector.

The aim of this paper is to analyze and to demonstrate stable optical rigidity in aLIGO (or Michelson-Sagnac interferometer with PRM and SRM) a) pumped through PRM, b) with arm detuning as small as possible (hence, small output power through SRM). This result may be applied not only to large-scale gravitational-wave detectors [34] but also to other optomechanical systems like micro-membranes inside optical cavities [35] (see Fig. 2), micro-toroids [36], optomechanical crystals [37], pulse-pumped optomechanical cavities [38]. In spite of the fact that optical rigidity, introduced into micromechanical oscillators, is relatively small as compared with the intrinsic one [31], it may be used for control and manipulation of its dynamics.

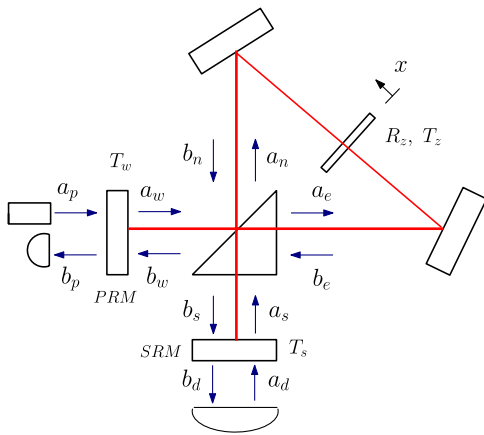


FIG. 2 (color online). Michelson-Sagnac interferometer with power and signal recycling mirrors (PRM and SRM). Middle mirror with amplitude reflectivity R_z may move as a free mass.

II. DESCRIPTION OF MODEL

We consider a gravitational-wave antenna aLIGO shown in Fig. 1, amplitude transmittances of SRM and PRM are T_s and T_w correspondingly. Antenna consists of a Michelson interferometer with additional mirrors forming Fabry-Perot (FP) cavities with mean distance L between mirrors in arms which is much larger than distances ℓ between beam splitter and SRM or PRM. Input mirrors have amplitude transmittance T and masses m , end mirrors have the same masses m and are completely reflective. Input and end mirrors in arms may move as free masses. We assume that all mirrors are lossless. The interferometer is pumped by laser through PRM.

Recall the dynamics of the pure balanced interferometer (i.e., identical FP cavities in arms tuned in resonance with pumped laser) can be split into two modes: namely symmetric and antisymmetric ones. Each mode is characterized by optical detuning δ_w (δ_s) and decay rate γ_w (γ_s) dependent on displacement and transparency of PRM for symmetric mode (SRM for antisymmetric one correspondingly). Here and below we denote detuning as the difference between laser frequency ω_0 and eigenfrequencies $\omega_{w,s}$ of symmetric and antisymmetric modes:

$$\delta_w = \omega_0 - \omega_w, \quad \delta_s = \omega_0 - \omega_s. \quad (1)$$

(In aLIGO PRM detuning δ_w is assumed to be zero, however, below we reserve possibility to vary it.) The optical fields in the modes represent difference (e_-) and sum (e_+) of the fields in arms, respectively, and carry information about difference (z_-) and sum (z_+) between lengths of arm cavities,

$$e_{\pm} = \frac{e_e \pm e_n}{\sqrt{2}}, \quad (2)$$

$$z_{\pm} = \frac{z_e \pm z_n}{2}, \quad z_{e,n} \equiv x_{e,n} - y_{e,n}, \quad (3)$$

(see notations in Fig. 1). In turn, light pressure force may be divided into two part: fluctuational one responsible for fluctuational back action and regular part creating optical spring [39]. Below we analyze the simplified case when sum mechanical displacement is fixed (for example, by feedback):

$$z_+ = 0. \quad (4)$$

When FP cavities in arms are detuned by $\pm\delta$ symmetric and antisymmetric modes became coupled with each other. In this case detunings δ_w, δ_s (1) and decay rates γ_w, γ_s refer to partial modes. As a result, the system is described by linear set of equations for Fourier components of fields $e_{\pm}(\Omega)$, $e_{\pm}^{\dagger}(-\Omega)$ and displacement $z_-(\Omega)$:

$$\begin{aligned}
 (\gamma_w - i\delta_w - i\Omega)e_+(\Omega) - i\delta e_-(\Omega) - \frac{ik}{\tau}E_{-z_-}(\Omega) \\
 = \frac{\sqrt{\gamma_w}g_p(\Omega)}{\sqrt{\tau}}, \tag{5a}
 \end{aligned}$$

$$\begin{aligned}
 -i\delta e_+(\Omega) + (\gamma_s - i\delta_s - i\Omega)e_-(\Omega) - \frac{ik}{\tau}E_{+z_-}(\Omega) \\
 = \frac{\sqrt{\gamma_s}g_d(\Omega)}{\sqrt{\tau}}, \tag{5b}
 \end{aligned}$$

$$\begin{aligned}
 (\gamma_w + i\delta_w - i\Omega)e_+^\dagger(-\Omega) + i\delta e_-^\dagger(-\Omega) + \frac{ik}{\tau}E_{-z_-}^*(\Omega) \\
 = \frac{\sqrt{\gamma_w}g_p^\dagger(-\Omega)}{\sqrt{\tau}}, \tag{5c}
 \end{aligned}$$

$$\begin{aligned}
 i\delta e_+^\dagger(-\Omega) + (\gamma_s + i\delta_s - i\Omega)e_-^\dagger(-\Omega) + \frac{ik}{\tau}E_{+z_-}^*(\Omega) \\
 = \frac{\sqrt{\gamma_s}g_d^\dagger(-\Omega)}{\sqrt{\tau}}, \tag{5d}
 \end{aligned}$$

$$\begin{aligned}
 \hbar k\{E_+^*e_-(\Omega) + E_-^*e_+(\Omega) + E_+e_-^\dagger(-\Omega) + E_-e_+^\dagger(-\Omega)\} \\
 + \mu\Omega^2z_-(\Omega) = 0, \tag{5e}
 \end{aligned}$$

$$\begin{aligned}
 k \equiv \frac{\omega_0}{c}, \quad \tau \equiv \frac{L}{c}, \quad \mu \equiv \frac{m}{2}, \quad E_- \equiv \xi E_+, \\
 \xi \equiv \frac{i\delta}{\gamma_s - i\delta_s}, \quad I_+ = \hbar\omega_0|E_+|^2. \tag{5f}
 \end{aligned}$$

Here \hbar is Plank constant, k is wave vector corresponding to laser wave frequency ω_0 , c is speed of light. E_\pm are mean complex amplitudes of symmetric and antisymmetric modes (excited by pump laser), I_+ is power circulating in symmetric mode. The right parts ($g_{p,d}(\Omega)$, $g_{p,d}^\dagger(-\Omega)$) in set describe vacuum fields incoming into interferometer through PRM and SRM. Details of notations and derivation are presented in Appendix A.

In spite of the fact that set (5) is not convenient for analysis of sensitivity (because we have to recalculate fields e_\pm into output field in the signal port), however, it is convenient for optical rigidity analysis.

Following oscillations theory advises we rewrite (5) introducing normal coordinates $b_\pm(\Omega)$, $b_\pm^\dagger(-\Omega)$ for e.m. fields and new (complex) eigenvalues λ_\pm :

$$(-i\Omega - \lambda_+)b_+(\Omega) - iz_-[\xi - \chi] = 0 \tag{6a}$$

$$(-i\Omega - \lambda_-)b_-(\Omega) - iz_-[1 + \chi\xi] = 0, \tag{6b}$$

$$(-i\Omega - \lambda_+^*)b_+^\dagger(-\Omega) + iz_-[\xi^* - \chi^*] = 0 \tag{6c}$$

$$(-i\Omega - \lambda_-^*)b_-^\dagger(-\Omega) - iz_-[1 + \chi^*\xi^*] = 0, \tag{6d}$$

$$\begin{aligned}
 \frac{b_+(\Omega)[\xi^* - \chi] + b_-(\Omega)[1 + \xi^*\chi]}{d} \\
 + \frac{b_+^\dagger(-\Omega)[\xi + \chi^*] + b_-^\dagger(-\Omega)[1 + \xi\chi^*]}{d^*} + \frac{\Omega^2}{J_+}z_- = 0, \tag{6e}
 \end{aligned}$$

$$b_+(\Omega) = \sqrt{\frac{\hbar L^2}{\omega I_+}}[e_+(\Omega) - \chi e_-(\Omega)], \tag{6f}$$

$$b_-(\Omega) = \sqrt{\frac{\hbar L^2}{\omega I_+}}[\chi e_+(\Omega) + e_-(\Omega)]. \tag{6g}$$

Here we introduce the following notations:

$$\lambda_\pm = -(\Gamma_+ \pm \Gamma_- \sqrt{1 + \Delta^2}), \quad J_+ \equiv \frac{kI_+}{L\mu}, \tag{7}$$

$$\Gamma_\pm \equiv \frac{\gamma_w - i\delta_w \pm (\gamma_s - i\delta_s)}{2}, \quad d \equiv 1 + \chi^2, \tag{8}$$

$$\chi \equiv \frac{i\delta}{\Gamma_w + \lambda_-} = \frac{\Delta}{1 + \sqrt{1 + \Delta^2}}, \quad \Delta \equiv \frac{i\delta}{\Gamma_-}. \tag{9}$$

In set (6) we omit fluctuational fields in right parts as we are interested in the dynamic behavior of system, i.e., in eigenvalues of the determinant.

After substitution ($-i\Omega \rightarrow \lambda$) characteristic equation of set (6) may be written in form:

$$\lambda^2 + \frac{\mathcal{I}_1[1 + \alpha_1(\lambda + \tilde{\gamma}_s)]}{(\lambda + \tilde{\gamma}_s)^2 + \tilde{\delta}_s^2} + \frac{\mathcal{I}_2[1 + \alpha_2(\lambda + \tilde{\gamma}_w)]}{(\lambda + \tilde{\gamma}_w)^2 + \tilde{\delta}_w^2} = 0, \tag{10}$$

where we introduce the following notations:

$$\tilde{\gamma}_{w,s} \equiv -\Re\lambda_\pm, \quad \tilde{\delta}_{w,s} \equiv \Im\lambda_\pm, \tag{11a}$$

$$\mathcal{I}_1 \equiv \frac{2J_+\tilde{\delta}_s\Re\phi}{|d|^2}, \quad \alpha_1 \equiv \frac{\Im\phi}{\tilde{\delta}_s\Re\phi}, \tag{11b}$$

$$\mathcal{I}_2 \equiv \frac{2J_+\tilde{\delta}_w\Re\psi}{|d|^2}, \quad \alpha_2 \equiv \frac{\Im\psi}{\tilde{\delta}_w\Re\psi}, \tag{11c}$$

$$\phi \equiv (1 + \xi^*\chi)(1 + \chi\xi)d^*, \tag{11d}$$

$$\psi \equiv (\xi^* - \chi)(\xi - \chi)d^*. \tag{11e}$$

The form of equation (10) is the same as for double pumped optical spring [27,28]: two fractions ($\sim\mathcal{I}_1$ and $\sim\mathcal{I}_2$) are similar to two optical springs created in two optical modes pumped separately. This analogy has physical sense—for imbalanced interferometer one pump excites two normal modes. This analogy became more obvious when relaxation rates of symmetric and antisymmetric modes are equal

($\gamma_w = \gamma_s$). In this case the values κ and ξ are pure real and $\alpha_1 = \alpha_2 = 0$. Then characteristic equation takes the following form:

$$\lambda^2 + \frac{\mathcal{I}_1}{(\lambda + \tilde{\gamma}_s)^2 + \tilde{\delta}_s^2} + \frac{\mathcal{I}_2}{(\lambda + \tilde{\gamma}_w)^2 + \tilde{\delta}_w^2} = 0 \quad (12)$$

Note that practically the same set as (5) is valid for Michelson-Sagnac interferometer shown in Fig. 2—see details in Appendix B. In particular, the equation (10) is valid after following substitutions:

$$\delta^2 \rightarrow R_z^2 \delta^2, \quad J_+ \rightarrow R_z^2 J_+, \quad \mu \rightarrow m, \quad (13)$$

where R_z is amplitude reflectivity of middle mirror, m is its mass.

III. ANALYSIS

Eq. (10) may be written in form convenient for further approximation

$$D_1^{(0)} D_2^{(0)} + D^{(1)} = 0, \quad (14)$$

$$D_1^{(0)} = [\lambda^2((\lambda + \tilde{\gamma}_s)^2 + \tilde{\delta}_s^2) + \mathcal{I}_1(1 + \alpha_1(\lambda + \tilde{\gamma}_s))], \quad (15)$$

$$D_2^{(0)} = [(\lambda + \tilde{\gamma}_w)^2 + \tilde{\delta}_w^2], \quad (16)$$

$$D^{(1)} = [(\lambda + \tilde{\gamma}_s)^2 + \tilde{\delta}_s^2] \mathcal{I}_2 (1 + \alpha_2(\lambda + \tilde{\gamma}_w)). \quad (17)$$

Underline that Eq. (14) is still exact characteristic equation. Mathematically its left part is a polynomial of 6-th degree relatively variable λ . Its solution provides set of eigenvalues λ_k , its imaginary parts describe eigenfrequencies whereas real parts—relaxation rates (positive one corresponds to instability). It is not difficult task for numerical solution of (14) using contemporary mathematical packets. However, analysis based on numeric calculations is not simple because there is set of 6 parameters ($\gamma_{w,s}$, $\delta_{w,s}$, δ , I_+) which may be varied.

In theoretical analysis below we make following assumptions:

(i) Interferometer is pumped through PRM.

(ii) Arm detuning is small: $\delta \ll \delta_{w,s}$.

(iii) Initial relaxation rates are small: $\gamma_{w,s} \ll \delta_{w,s}$.

Then Eq. (14) may be solved by iteration method considering term $D_1^{(0)} D_2^{(0)}$ as main term (in zero approximation roots are $\lambda_k^{(0)}$), whereas account of term $D^{(1)}$ of first order of smallness gives next iteration $\lambda_k^{(1)}$. We can do that because coefficients $\xi, \kappa \sim \delta$ (5f,9), hence, $\psi \sim \delta^2$ (11e) and the “additional” pump $\mathcal{I}_2 \sim \delta^2$ (11c). It means that \mathcal{I}_2 is much smaller than the “main” pump \mathcal{I}_1 and we may apply iteration method.

Zero order iteration.—The solution of equation $D_1^{(0)} = 0$ is following:

$$\lambda_{1,2}^{(0)} = \gamma_1 \pm i\delta_1, \quad \lambda_{3,4}^{(0)} = \gamma_3 \pm i\delta_3 \quad (18)$$

$$\begin{aligned} \gamma_1 &\equiv \frac{\tilde{\gamma}_s(1-p) - (1-p^2)\beta_1}{2p}, & \delta_1 &\equiv \sqrt{\frac{\tilde{\gamma}_s^2 + \tilde{\delta}_s^2}{2}}(1-p), \\ \gamma_3 &\equiv -\frac{\tilde{\gamma}_s(1+p) - (1-p^2)\beta_1}{2p}, & \delta_3 &\equiv \sqrt{\frac{\tilde{\gamma}_s^2 + \tilde{\delta}_s^2}{2}}(1+p), \\ p &\equiv \sqrt{1 - \frac{4\mathcal{I}_1(1 + \alpha_1\tilde{\gamma}_s)}{[\tilde{\gamma}_s^2 + \tilde{\delta}_s^2]^2}}, & \beta_1 &\equiv \frac{\alpha_1(\tilde{\gamma}_s^2 + \tilde{\delta}_s^2)}{4(1 + \alpha_1\tilde{\gamma}_s)} \end{aligned} \quad (19)$$

Note that in the case of zero arm detuning ($\delta = 0$) these roots was found earlier [18,21,22] (for example, the case of $p = 0$ corresponds to double resonance regime) and formulas above may be considered as generalization for small δ .

Solution of equation $D_2^{(0)} = 0$ gives obvious roots:

$$\lambda_{5,6}^{(0)} = -\tilde{\gamma}_w \pm i\tilde{\delta}_w. \quad (20)$$

So in zero-order approximation we have roots $\lambda_k^{(0)}$, among them the roots $\lambda_{1,2}^{(0)}$ correspond to instability ($\gamma_1 > 0$). Now the zero-order part of the determinant may be written as

$$\begin{aligned} D_1^{(0)} D_2^{(0)} &= [(\lambda - \gamma_1)^2 + \delta_1^2][(\lambda - \gamma_3)^2 + \delta_3^2] \\ &\quad \times [(\lambda + \tilde{\gamma}_w)^2 + \tilde{\delta}_w^2]. \end{aligned} \quad (21)$$

First order of iteration.—Our aim is to choose such parameters that make stable the next iteration root $\lambda_{1,2}^{(1)}$, i.e.,

$$\Re[\lambda_{1,2}^{(1)}] < 0. \quad (22)$$

We divide (14) by $[(\lambda - \gamma_3)^2 + \delta_3^2]$ [taking into account (21)] and put $\lambda = \lambda_{1,2}^{(0)}$ in $D^{(1)}$. So we get the next iteration of the following characteristic equation:

$$((\lambda - \gamma_1)^2 + \delta_1^2)((\lambda + \tilde{\gamma}_w)^2 + \tilde{\delta}_w^2) - b = 0, \quad (23)$$

$$b \equiv \frac{D^{(1)}}{(\lambda - \gamma_3)^2 + \delta_3^2} \Big|_{\lambda = \lambda_{1,2}^{(0)}}. \quad (24)$$

We may keep in mind that b is a constant of the first order of smallness.

Below we put $\tilde{\delta}_w \approx -\delta_1$. It is this choice of $\tilde{\delta}_w$ that provides stability with minimal arm detuning δ . This choice has physical sense corresponding to the scheme of laser cooling (see, for example [40,41]). Indeed, let the FP cavity, which one mirror is a mechanical oscillator with frequency ω_m , is pumped by laser with frequency less than cavity frequency by ω_m detuned from resonance. In this

case positive damping will be created for movement of mechanical oscillator (optical rigidity is negligibly small).

One may write down the solution of (23) in analytical form:

$$\lambda = \frac{\gamma_1 - \tilde{\gamma}_w}{2} \pm i\sqrt{\delta_1^2 - \left[\frac{\gamma_1 + \tilde{\gamma}_w}{2}\right]^2} \pm \sqrt{b - \delta_1^2[\gamma_1 + \tilde{\gamma}_w]^2}. \quad (25)$$

Analysis shows that $\Re b \ll \Im b$. Then at condition

$$\Re b = \delta_1^2[\gamma_1 + \tilde{\gamma}_w]^2, \quad (26)$$

the second term in (25) is practically imaginary and its real part is small enough. Then the condition stability may be approximately formulated as

$$\tilde{\gamma}_w > \gamma_1, \quad \text{or} \quad \tilde{\gamma}_w > \tilde{\gamma}_s \frac{1-p}{2p}. \quad (27)$$

This condition gives an estimation for the minimal value of arm detuning:

$$\delta^2 > \left[\tilde{\gamma}_s \frac{1-p}{2p} + \tilde{\gamma}_w \right]^2 \times \left(\frac{\sqrt{2} + \sqrt{1-p}}{2\sqrt{2} + \sqrt{1-p}} \right)^2 \frac{4\sqrt{2}p}{(1-p)^{1/2}(1+p)^2}. \quad (28)$$

The formula (28) is confirmed by numerical calculations presented in the following section.

Important that in order to fulfill condition (28) one has to provide relatively small arm detuning $\delta \sim \tilde{\gamma}_w$. Here we made an assumption that $\tilde{\gamma}_{w,s}$ depend weakly on a value of δ . So we put $\tilde{\gamma}_{w,s} \approx \gamma_{w,s}$ correspondingly when doing numerical estimations, because otherwise (28) turns into a nontrivial equation for δ (we did this approximation only estimating value of δ , other numerical calculations stay exact).

IV. NUMERICAL ESTIMATIONS

Numerical estimations can serve as an examination of our theory. We can solve (14) numerically substituting realistic parameters. We chose the parameters for aLIGO interferometer presented in Table I [42]. We consider two cases—when $\tilde{\gamma}_w \neq \tilde{\gamma}_s$ and when $\tilde{\gamma}_w = \tilde{\gamma}_s$. In the Table values in brackets mean the second case. Our analysis

TABLE I. Parameters for aLIGO

Detuning of symmetric mode (δ_w)	-23.0 Hz
Detuning of antisymmetric mode (δ_s)	42.4 Hz
Decay rate of symmetric mode (γ_w)	1.5 Hz (3.0 Hz)
Decay rate of antisymmetric mode (γ_s)	0.3 Hz (3.0 Hz)
Test mass (m)	40 kg
Arm length (L)	4 km
Circulating power (I_{circ})	24 kW
Arm detuning (δ)	1.51 Hz (4.6 Hz)

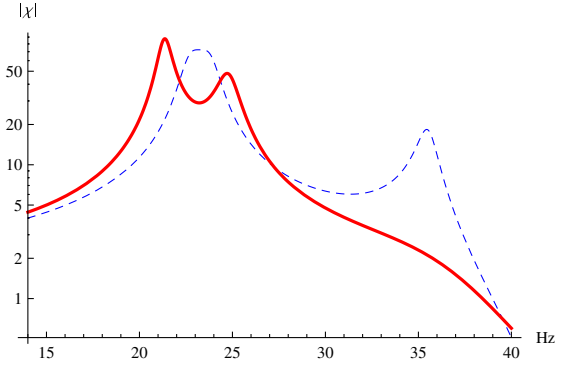


FIG. 3 (color online). Absolute value of susceptibility χ of aLIGO interferometer with excluded symmetric mechanical mode. Red continuous curve: $\tilde{\gamma}_w = \tilde{\gamma}_s$. Blue dashed curve: $\tilde{\gamma}_w \neq \tilde{\gamma}_s$.

also gives an estimation for output power $I_{\text{out}} = 0.03\text{W}$ (as we know in aLIGO reference design output power should be about 0.1W). It is a good result because we don't want to obtain big laser power on a photodetector. Importantly that here we chose operating frequency about 30 Hz. This value differs from aLIGO one—100 Hz. We made it because in our case the power-recycling mirror is detuned from resonance. From this fact it follows that the circulating power ($\sim 24\text{ kW}$) is less than in aLIGO ($\sim 800\text{ kW}$). Susceptibility curves for these parameters are represented in Fig. 3. The numerical solution of (14) gives us a set of eigenvalues with negative real parts, which means stability. It is important that the numerical eigenvalues are in good agreement with analytical estimates. In addition we checked our analysis numerically by the Routh-Hurwitz stability criterion. It showed stability for parameters predicted by our theory.

We also did the same analysis for the Michelson-Sagnac interferometer. For such systems we chose the realistic parameters presented in Table II [30,31]. However, we consider membrane as a free mass not taking into account its intrinsic rigidity. The numerical solution gives us a set of eigenvalues with negative real parts again. Plots of susceptibilities are represented in Fig. 4.

Our analysis shows that we can control the shape of the susceptibility curve (increase one peak and decrease another one) just detuning $\tilde{\delta}_w$ by small value Δ from the

TABLE II. Parameters for Michelson-Sagnac interferometer.

Detuning of symmetric mode (δ_w)	-77.2 kHz
Detuning of antisymmetric mode (δ_s)	141.0 kHz
Decay rate of symmetric mode (γ_w)	5 kHz (10 kHz)
Decay rate of antisymmetric mode (γ_s)	1 kHz (10 kHz)
Test mass (m)	10^{-10} kg
Arm length (L)	8.7 cm
Circulating power (I_{circ})	318 mW
Arm detuning (δ)	5 kHz (15 kHz)
Membrane reflectivity (R_z^2)	0.17

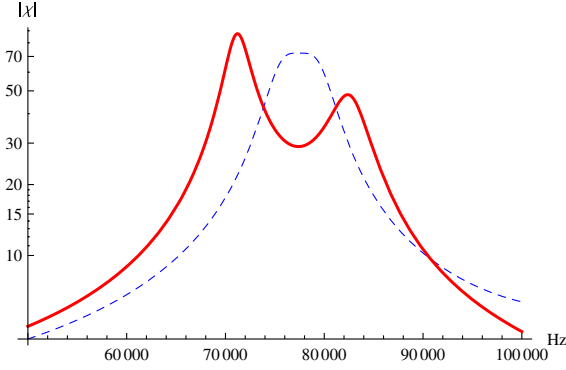


FIG. 4 (color online). Absolute value of susceptibility χ of Michelson-Sagnac interferometer. Red continuous curve: $\tilde{\gamma}_w = \tilde{\gamma}_s$. Blue dashed curve: $\tilde{\gamma}_w \neq \tilde{\gamma}_s$.

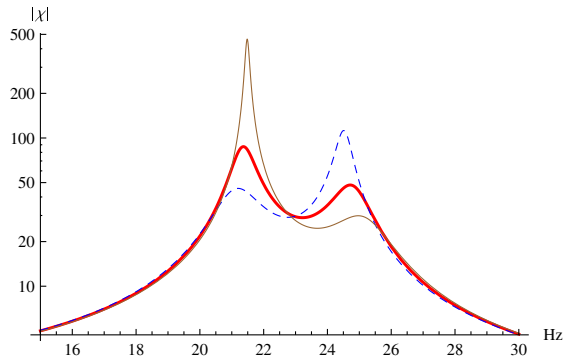


FIG. 5 (color online). Absolute value of susceptibility χ of aLIGO with $\tilde{\delta}_w = -\delta_1 + \Delta$. Red thick curve: $\Delta = 0$. Blue dashed curve: $\Delta = 0.5$ Hz. Brown thin curve: $\Delta = -0.5$ Hz

optimal one: $\tilde{\delta}_w = -\delta_1 + \Delta$. In Fig. 5 we plot such curves for parameters represented in Table. I.

V. CONCLUSION

We have shown that arm detuning δ in the aLIGO interferometer provides the possibility to make a stable optical spring for the antisymmetric mechanical mode. It is important that the stable optical spring may be created with small arm detuning comparable with the optical bandwidths: $\delta \approx \gamma_w, \gamma_s$. However, this regime requires relatively large PR and SR detunings which restrict power circulating in the arms of the interferometer. These results may be easily applied to the Michelson-Sagnac interferometer with membrane inside to create stable optical spring.

We restrict ourselves by analysis of only the antisymmetric mechanical mode in the detuned aLIGO interferometer. In further research we plan to answer the following question: is it possible to make both the symmetric and antisymmetric mechanical modes stable?

ACKNOWLEDGMENTS

We are grateful to R. Adhikari, Y. Chen, H. Miao, F. Khalili, and especially to S. Tarabrin for fruitful discussions. The authors are supported by the Russian Foundation for Basic Research Grants No. 08-02-00580-a, No. 13-02-92441 and by NSF Grant No. PHY-1305863.

APPENDIX A: NOTATIONS AND DERIVATION OF INITIAL EQUATIONS

Here we explain notations and derive a set of equations (5), describing the aLIGO scheme represented in Fig. 1.

The electrical field E of the optical wave is presented in a standard way,

$$E = \sqrt{\frac{2\pi\hbar\omega_0}{Sc}} e^{-i\omega_0 t} (A + a_{\text{fl}}) + \text{H.c.}$$

$$a_{\text{fl}} = \int_0^\infty \sqrt{\frac{\omega}{\omega_0}} a(\omega) e^{-i(\omega-\omega_0)t} \frac{d\omega}{2\pi}, \quad (\text{A1})$$

where A is the mean amplitude, ω_0 is the mean frequency (mean power P of traveling wave is $P = \hbar\omega_0 |A|^2$), the $a(\omega)$ operators describe quantum fluctuations, and their commutators are

$$[a(\omega), a^\dagger(\omega')] = 2\pi\delta(\omega - \omega'). \quad (\text{A2})$$

Usually the fluctuation part is written in form

$$a_{\text{fl}} \approx \int_{-\infty}^\infty a(\Omega) e^{-i\Omega t} \frac{d\Omega}{2\pi}, \quad (\text{A3})$$

where $\Omega = \omega - \omega_0$ (see details in [43]). We assume that input wave is in coherent state. In this case we have the following averages:

$$\langle a(\Omega) a^\dagger(\Omega') \rangle = 2\pi\delta(\Omega - \Omega'), \quad \langle a^\dagger(\Omega') a(\Omega) \rangle = 0. \quad (\text{A4})$$

In our notations we use big letters for mean (classical) part of field and small letters for small additions including quantum fluctuating component.

1. The beamsplitter

For incident and reflected fields on beam splitter we assume following formulas

$$b_w = -\frac{b_e + b_n}{\sqrt{2}}, \quad a_b = -\frac{b_e - b_n}{\sqrt{2}}, \quad (\text{A5a})$$

$$a_e = -\frac{a_w + a_s}{\sqrt{2}}, \quad a_n = -\frac{a_w - a_s}{\sqrt{2}}. \quad (\text{A5b})$$

2. Mean fields

For reflected fields of east and north cavities we can write:

$$B_e = \mathcal{R}_e A_e, \quad B_n = \mathcal{R}_n A_n, \quad (\text{A6})$$

The both east and north arms are assumed to be slightly detuned by δ from resonance to opposite sides. We introduce following notations and calculate generalized reflectivities $\mathcal{R}_e, \mathcal{R}_n$ in long way approximation:

$$\Theta_e = e^{-i\delta\tau}, \quad \Theta_n = e^{i\delta\tau}, \quad \delta = \omega_0 - \omega_{\text{res}}, \quad (\text{A7})$$

$$\begin{aligned} \gamma_T &= \frac{T^2}{4\tau}, & \tau &= \frac{L}{c}, \\ \mathcal{R}_e &\equiv \frac{\gamma_T + i\delta}{\gamma_T - i\delta} = \mathcal{R}_n^*, & \mathcal{R}_n &\equiv \frac{\gamma_T - i\delta}{\gamma_T + i\delta}. \end{aligned} \quad (\text{A8})$$

Using (A5) we get

$$A_e = -(A_w + A_s)/\sqrt{2}, \quad B_e = \mathcal{R}_e A_e \quad (\text{A9a})$$

$$A_n = -(A_w - A_s)/\sqrt{2}, \quad B_n = \mathcal{R}_n A_n \quad (\text{A9b})$$

$$B_w = -(B_e + B_n)/\sqrt{2} = A_w \mathcal{R}_+ + A_s \mathcal{R}_-, \quad (\text{A9c})$$

$$B_s = -(B_e - B_n)/\sqrt{2} = A_w \mathcal{R}_- + A_s \mathcal{R}_+, \quad (\text{A9d})$$

where we introduced $\mathcal{R}_\pm \equiv \frac{\mathcal{R}_e \pm \mathcal{R}_n}{2}$,

$$\mathcal{R}_+ = \frac{\gamma_+ \gamma_- - \delta^2}{\gamma_+^2 + \delta^2}, \quad \mathcal{R}_- = \frac{i\delta(\gamma_+ + \gamma_-)}{\gamma_+^2 + \delta^2}. \quad (\text{A10a})$$

Now we may consider the SR (south) and PR (west) cavities which are described by equations (keep in mind that there is no pumping into the south arm, but keeping A_d yet):

$$B_p = -R_w A_p + iT_w \Theta_w B_w, \quad (\text{A11a})$$

$$A_w = -R_w \Theta_w^2 B_w + iT_w \Theta_w A_p, \quad (\text{A11b})$$

$$B_d = iT_s \Theta_s B_s - R_s A_d, \quad (\text{A11c})$$

$$A_s = -R_s \Theta_s^2 B_s + iT_s \Theta_s A_d, \quad (\text{A11d})$$

$$\Theta_{w,s} \equiv e^{i\omega_0 \tau_{w,s}}. \quad (\text{A11e})$$

Using (A9) one may write set of linear equations (A11b), (A11d) for A_s and A_w which may be solved for nonzero A_d :

$$A_w(1 + R_w \Theta_w^2 \mathcal{R}_+) + A_s R_w \Theta_w^2 \mathcal{R}_- = iT_w \Theta_w A_p, \quad (\text{A12})$$

$$A_w R_s \Theta_s^2 \mathcal{R}_- + A_s(1 + R_s \Theta_s^2 \mathcal{R}_+) = iT_s \Theta_s A_d. \quad (\text{A13})$$

Solving this set and simplifying the solution one gets

$$\begin{aligned} A_w &= \frac{iA_p \sqrt{\gamma_w/\gamma_T} e^{i\alpha_w} (\gamma_+ \Gamma_s + \delta^2)}{\Gamma_s \Gamma_w + \delta^2} \\ &\quad - \frac{iA_d \sqrt{\gamma_s/\gamma_T} e^{i\alpha_s} 2i\delta \gamma_T R_w \Theta_w^2}{(\Gamma_s \Gamma_w + \delta^2)(1 - R_w \Theta_w^2)}, \end{aligned} \quad (\text{A14})$$

$$\begin{aligned} A_s &= \frac{iA_d \sqrt{\gamma_s/\gamma_T} e^{i\alpha_s} (\gamma_+ \Gamma_w + \delta^2)}{\Gamma_s \Gamma_w + \delta^2} \\ &\quad - \frac{iA_p \sqrt{\gamma_w/\gamma_T} e^{i\alpha_w} 2i\delta \gamma_T R_s \Theta_s^2}{(\Gamma_s \Gamma_w + \delta^2)(1 - R_s \Theta_s^2)}, \end{aligned} \quad (\text{A15})$$

where we introduced the following notations:

$$\Gamma_{s,w} \equiv \gamma_{s,w} - i\delta_{s,w} \equiv \frac{\gamma_+ + \gamma_- R_{s,w} \Theta_{s,w}^2}{1 - R_{s,w} \Theta_{s,w}^2} \quad (\text{A16})$$

$$\gamma_{s,w} = \frac{\gamma_T(1 - R_{s,w}^2)}{|1 - R_{s,w} \Theta_{s,w}^2|^2}, \quad (\text{A17})$$

$$\delta_{s,w} \equiv - \left[\frac{\gamma_+ + \gamma_-}{2} \right] \frac{R_{s,w} [\Theta_{s,w}^2 - \Theta_{s,w}^{*2}]}{|1 - R_{s,w} \Theta_{s,w}^2|^2},$$

$$e^{i\alpha_{s,w}} \equiv \frac{\Theta_{s,w} |1 - R_{s,w} \Theta_{s,w}^2|}{1 - R_{s,w} \Theta_{s,w}^2} = \sqrt{\frac{\Theta_{s,w}^2 - R_s}{1 - R_{s,w} \Theta_{s,w}^2}}. \quad (\text{A18})$$

Now we can calculate fields before input mirrors in arms using (A14), (A15) and (A11):

$$\begin{aligned} A_e &= - \frac{i\sqrt{\gamma_w/\gamma_T} A_p e^{i\alpha_w} (\gamma_+ - i\delta)(\Gamma_s + i\delta)}{\sqrt{2}(\Gamma_s \Gamma_w + \delta^2)} \\ &\quad - \frac{i\sqrt{\gamma_s/\gamma_T} A_d e^{i\alpha_s} (\gamma_+ - i\delta)(\Gamma_w + i\delta)}{\sqrt{2}(\Gamma_s \Gamma_w + \delta^2)}, \end{aligned} \quad (\text{A19})$$

$$\begin{aligned} A_n &= - \frac{i\sqrt{\gamma_w/\gamma_T} A_p e^{i\alpha_w} (\gamma_+ + i\delta)(\Gamma_s - i\delta)}{\sqrt{2}(\Gamma_s \Gamma_w + \delta^2)} \\ &\quad + \frac{i\sqrt{\gamma_s/\gamma_T} A_d e^{i\alpha_s} (\gamma_+ + i\delta)(\Gamma_w - i\delta)}{\sqrt{2}(\Gamma_s \Gamma_w + \delta^2)}. \end{aligned} \quad (\text{A20})$$

And finally we calculate mean fields circulating in arms:

$$E_{e,n} = \mathcal{T}_{e,n} A_{e,n}, \quad \mathcal{T}_{e,n} = \frac{i\sqrt{\gamma_T/\tau}}{\gamma_+ \mp i\delta}, \quad (\text{A21})$$

$$E_\pm = (E_e \pm E_n)/\sqrt{2} \quad (\text{A22})$$

$$E_+ = \frac{\sqrt{\gamma_w/\tau} A_p e^{i\alpha_w} \Gamma_s}{(\Gamma_s \Gamma_w + \delta^2)} + \frac{\sqrt{\gamma_s/\tau} A_d e^{i\alpha_s} i\delta}{(\Gamma_s \Gamma_w + \delta^2)}, \quad (\text{A23})$$

$$E_- = \frac{\sqrt{\gamma_w/\tau} A_p e^{i\alpha_w} i\delta}{(\Gamma_s \Gamma_w + \delta^2)} + \frac{\sqrt{\gamma_s/\tau} A_d e^{i\alpha_s} \Gamma_w}{(\Gamma_s \Gamma_w + \delta^2)}. \quad (\text{A24})$$

3. Small fields

Below we consider small (and fluctuative) part of a field in frequency domain. The logic of derivation is the same, but in this situation fluctuative part contains information on spectral frequency Ω .

a. East and north arms

We use long-wavelength approximation for the arm cavity. In particular, we assume that the field reflected from the arm contains information on difference coordinates $z_{e,n}$ of the arm. So we assume that $b_{n,e}$ and $a_{n,e}$ may be expressed by formulas:

$$b_{e,n} = a_{e,n} \mathbb{R}_{e,n} - E_{e,n} \mathbb{T}_{e,n} 2ikz_{e,n}, \quad (\text{A25a})$$

$$e_{e,n} = a_{e,n} \mathbb{T}_{e,n} - E_{e,n} \frac{\mathbb{T}_{e,n}}{iT} 2ikz_{e,n}, \quad (\text{A25b})$$

$$\mathbb{R}_e = \frac{\gamma_T + i(\delta + \Omega)}{\gamma_T - i(\delta + \Omega)}, \quad \mathbb{R}_n = \frac{\gamma_T + i(\Omega - \delta)}{\gamma_T - i(\Omega - \delta)}, \quad (\text{A25c})$$

$$\mathbb{T}_e = \frac{i\sqrt{\gamma_T/\tau}}{\gamma_T - i(\delta + \Omega)}, \quad \mathbb{T}_n = \frac{i\sqrt{\gamma_T/\tau}}{\gamma_T - i(\Omega - \delta)}, \quad (\text{A25d})$$

$$z_{n,e} = x_{n,e} - y_{n,e}. \quad (\text{A25e})$$

b. Beamsplitter

Now we may calculate using (A9)

$$a_e = -\frac{a_w + a_s}{\sqrt{2}}, \quad a_n = -\frac{a_w - a_s}{\sqrt{2}}, \quad (\text{A26a})$$

$$b_s = -\frac{b_e - b_n}{\sqrt{2}} = a_w \mathbb{R}_- + a_s \mathbb{R}_+ + Z_s, \quad (\text{A26b})$$

$$b_w = -\frac{b_e + b_n}{\sqrt{2}} = a_w \mathbb{R}_+ + a_s \mathbb{R}_- + Z_w, \quad (\text{A26c})$$

where we introduced following notations:

$$Z_s = \mathbb{T}_- W_- + \mathbb{T}_+ W_\times \quad (\text{A27})$$

$$Z_w = \mathbb{T}_+ W_- + \mathbb{T}_- W_\times, \quad (\text{A28})$$

$$W_- \equiv [E_+ z_+ + E_- z_-] 2ik, \quad (\text{A29})$$

$$W_\times \equiv [E_+ z_- + E_- z_+] i2k, \quad (\text{A30})$$

$$\mathbb{T}_+ \equiv \frac{\mathbb{T}_e + \mathbb{T}_n}{2} = \frac{i\sqrt{\gamma_T/\tau}(\gamma_T - i\Omega)}{(\gamma_T - i\Omega)^2 + \delta^2}, \quad (\text{A31})$$

$$\mathbb{T}_- \equiv \frac{\mathbb{T}_e - \mathbb{T}_n}{2} = \frac{i\sqrt{\gamma_T/\tau}i\delta}{(\gamma_T - i\Omega)^2 + \delta^2}, \quad (\text{A32})$$

$$z_\pm = \frac{z_e \pm z_n}{2}, \quad E_\pm = \frac{E_e \pm E_n}{\sqrt{2}}. \quad (\text{A33})$$

c. Inside fields in arms

Fields $e_{e,n}$ inside arms may be calculated using (A9) and (A25b). We may pass through sum and different fields $e_\pm = \frac{e_e \pm e_n}{\sqrt{2}}$. Instead of $\{a_d, a_p\}$ we may introduce the new basis for fluctuation amplitudes:

$$g_p = e^{i\alpha_w} a_p, \quad g_d = e^{i\alpha_s} a_d. \quad (\text{A34})$$

The fluctuational amplitudes $\{g_p, g_d\}$ are independent from each other as well as $\{a_d, a_p\}$, i.e., their cross correlators are equal to zero and own correlators are the same as for initial basis (see (A2))

$$[g_d(\Omega), g_d^\dagger(\Omega')] = 2\pi\delta(\Omega - \Omega'), \quad (\text{A35})$$

$$[g_p(\Omega), g_p^\dagger(\Omega')] = 2\pi\delta(\Omega - \Omega'). \quad (\text{A36})$$

After simple but bulky calculations we obtain expressions for e_\pm :

$$e_+ = \frac{[\Gamma_s - i\Omega]\sqrt{\gamma_w}g_p + i\delta\sqrt{\gamma_s}g_d}{\sqrt{\tau}[(\Gamma_s - i\Omega)(\Gamma_w - i\Omega) + \delta^2]} + \frac{W_-[\Gamma_s - i\Omega] + W_\times i\delta}{2\tau[(\Gamma_s - i\Omega)(\Gamma_w - i\Omega) + \delta^2]}, \quad (\text{A37a})$$

$$e_- = \frac{i\delta\sqrt{\gamma_w}g_p + [\Gamma_w - i\Omega]\sqrt{\gamma_s}g_d}{\sqrt{\tau}[(\Gamma_s - i\Omega)(\Gamma_w - i\Omega) + \delta^2]} + \frac{W_\times[\Gamma_w - i\Omega] + W_- i\delta}{2\tau[(\Gamma_s - i\Omega)(\Gamma_w - i\Omega) + \delta^2]}. \quad (\text{A37b})$$

We can rewrite formulas (A37) in form:

$$\begin{aligned} (\text{A37a}) \times (\Gamma_w - i\Omega) + (\text{A37b}) \times (-i\delta) \Rightarrow \\ (\Gamma_w - i\Omega)e_+ - i\delta e_- = \frac{\sqrt{\gamma_w}g_p}{\sqrt{\tau}} + \frac{ik(E_+ z_+ + E_- z_-)}{\tau}, \end{aligned} \quad (\text{A38})$$

$$\begin{aligned} (\text{A37b}) \times (\Gamma_s - i\Omega) + (\text{A37a}) \times (-i\delta) \Rightarrow \\ -i\delta e_+ + (\Gamma_s - i\Omega)e_- = \frac{\sqrt{\gamma_s}g_d}{\sqrt{\tau}} + \frac{ik(E_+ z_- + E_- z_+)}{\tau}. \end{aligned} \quad (\text{A39})$$

Equations (A38) and (A39) (and their complex conjugation) form first four equations of set (5) if we exclude symmetric mode (putting $z_+ = 0$).

d. Ponderomotive forces and equations of motion

We can express forces acting on end mirror in each arm in next way:

$$F_{e,n} = 2\hbar k(E_{e,n}^* e_{e,n} + E_{e,n} e_{e,n}^\dagger), \quad (\text{A40})$$

$$F_+ \equiv \frac{F_e + F_n}{2}, \quad F_- \equiv \frac{F_e - F_n}{2} \quad (\text{A41})$$

After that we can write equations of motion for symmetric and antisymmetric modes in frequency domain:

$$\hbar k[E_+^* e_-(\Omega) + E_-^* e_+(\Omega) + \{\text{h.c.}\}_-] + \mu\Omega^2 z_-(\Omega) = 0, \quad (\text{A42})$$

$$\hbar k[E_+^* e_+(\Omega) + E_-^* e_-(\Omega) + \{\text{h.c.}\}_+] + \mu\Omega^2 z_+(\Omega) = 0. \quad (\text{A43})$$

Equation (A42) forms last equation of set (5).

APPENDIX B: COMPARISON OF MICHELSON AND MICHELSON-SAGNAC INTERFEROMETERS

Here we prove the formulas (13). We consider simplified Michelson interferometer in Fig. 6, show that it is similar to aLIGO interferometer and it is described by set similar to (5). Then we consider Michelson-Sagnac interferometers and compare it with Michelson interferometer.

1. Michelson interferometer

Let us consider the Michelson interferometer without FP cavities in the arms but with power and signal recycling mirrors as shown in Fig. 6. It can be easily generalized in the case of aLIGO by redefining decay rates and detunings in this system.

The mirrors in the east and north arms may move as free masses, whereas the power and signal recycling mirrors in the west and south arms (with amplitude transmittances are T_w, T_s correspondingly) are assumed to be unmovable. The interferometer is pumped through the west port. For simplicity we assume that mean distance ℓ between beam splitter and recycling mirrors in west and south arms is much smaller than mean distance L between beam splitter and end mirrors in north and east arms: $\ell \ll L$.

In the case of complete balance optical paths in north and east arms are tuned so that whole output power returns through the power recycling mirror in the west arm and no average power goes through the signal recycling mirror in the south port. In this case one can analyze symmetric and

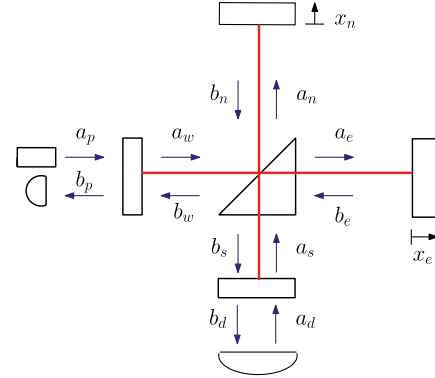


FIG. 6 (color online). Michelson interferometer with power and signal recycling mirrors.

antisymmetric modes separately, in particular, symmetric mode interact with symmetric mechanical mode ($x_e + x_n$) and antisymmetric one—with ($x_e - x_n$). We analyze the nonbalanced case when such separation is impossible.

Below for complex amplitudes of fields we use notations in Fig. 6 denoting by capital letters mean amplitudes and by small letters—small time-dependent additions.

It is easy to obtain equations for mean amplitudes A_w at the power recycling mirror and A_s at the signal recycling one:

$$A_w(1 - r_w \mathcal{R}_+) - A_s r_w \mathcal{R}_- = i e^{i\phi_w/2} T_w A_p, \quad (\text{B1a})$$

$$-A_w r_s \mathcal{R}_- + A_s(1 - r_s \mathcal{R}_+) = i e^{i\phi_s/2} T_s A_d, \quad (\text{B1b})$$

$$\mathcal{R}_+ = \cos \delta\tau, \quad \mathcal{R}_- = i \sin \delta\tau, \quad (\text{B1c})$$

$$\tau = 2L/c, \quad r_{w,s} = R_{w,s} e^{i\phi_{w,s}}. \quad (\text{B1d})$$

Here $R_{w,s}$ are amplitude reflectivities of the power and signal mirrors, respectively, τ is the round trip of light between the beam splitters and end mirrors, δ is the detuning introduced by displacements of the north and east mirrors (in opposite directions), $\phi_{s,w}$ is the round trip phase advance of the wave traveling between the beam splitter and the power (w) and signal (s) recycling mirrors, A_p is the mean amplitude of the pump laser, and for generality we add the term $\sim A_d$ describing the possible pump through the south port.

In the same way, one can obtain the equations for small amplitudes in the west and south arms in the frequency domain:

$$a_w[1 - r_w \mathcal{R}_+ e^{i\Omega\tau}] - a_s r_w \mathcal{R}_- e^{i\Omega\tau} = iT_w e^{i\phi_w/2} a_p + r_w ikX_w, \quad (\text{B2a})$$

$$-a_w r_s \mathcal{R}_- e^{i\Omega\tau} + a_s[1 - r_s \mathcal{R}_+ e^{i\Omega\tau}] = iT_s e^{i\phi_s/2} a_d + r_s ikX_s. \quad (\text{B2b})$$

Here Ω is the spectral frequency, and due to strong inequality $\ell \ll L$ we assume that phases $\phi_{w,s}$ do not depend on Ω . a_p, a_d describe the zero-point fluctuations of the input field, k is the wave vector, and values $X_{w,s}$ describe the influence of displacements x_e and x_n :

$$x_{\pm} \equiv x_e \pm x_n, \quad (\text{B3a})$$

$$X_w \equiv -e^{i\Omega\tau/2}(A_w\mathcal{R}_+ + A_s\mathcal{R}_-)x_+ - e^{i\Omega\tau/2}(A_w\mathcal{R}_- + A_s\mathcal{R}_+)x_-, \quad (\text{B3b})$$

$$X_s \equiv -e^{i\Omega\tau/2}(A_w\mathcal{R}_- + A_s\mathcal{R}_+)x_+ - e^{i\Omega\tau/2}(A_w\mathcal{R}_+ + A_s\mathcal{R}_-)x_-. \quad (\text{B3c})$$

In the long-wave approximation

$$\Omega\tau \ll 1, \quad \delta\tau \ll 1, \quad T_{w,s} \ll 1, \quad (\text{B4})$$

we have $\mathcal{R}_+ \simeq 1$, $\mathcal{R}_- \simeq i\delta\tau$ and may simplify set (B2) as follows,

$$a_w[\Gamma_w - i\Omega] - a_s i\delta = g_w, \quad (\text{B5a})$$

$$-a_w i\delta + a_s[\Gamma_s - i\Omega] = g_s, \quad (\text{B5b})$$

where

$$g_w \equiv \frac{iT_w a_p - r_w i k X_w}{\tau r_w}, \quad g_s \equiv \frac{iT_s a_d - r_s i k X_s}{\tau r_s} \\ X_w = -A_w x_+ - A_s x_-, \quad X_s = -A_w x_- - A_s x_+. \quad (\text{B6})$$

One can write down the following approximate formulas for Γ_w and Γ_s :

$$\Gamma_{w,s} \simeq \frac{1 - R_{w,s} e^{i\phi_{w,s}}}{\tau R_{w,s} e^{i\phi_{w,s}}} = \gamma_{w,s} - i\delta_{w,s}, \quad (\text{B7})$$

$$\gamma_{w,s} \simeq \frac{1 - R_{w,s} \cos \phi_{w,s}}{\tau}, \quad \delta_{w,s} \simeq \frac{\sin \phi_{w,s}}{\tau}. \quad (\text{B8})$$

In the case of zero detuning $\delta = 0$, the set (B5) transforms into equations of decoupled oscillators, whereas nonzero δ introduces coupling.

Importantly, the set (B5) may be recalculated to equations for $e_{\pm} \rightarrow -(a_e \pm a_n)/\sqrt{2}$, which are equivalent (with slightly different notations) to the first four equations in set (5). Here we have to introduce symmetric and antisymmetric modes with sign ‘‘minus’’ because the fields $a_{e,n}$ are defined near the beam splitter, whereas fields $e_{e,n}$ are defined near the end mirrors of the Fabry-Pero resonators.

Now we can write down equations for ponderomotive forces acting on the end mirrors of the interferometer. They can be expressed by the following formula:

$$F_e = 2\hbar k(A_e^* a_e + A_e a_e^\dagger), \quad (\text{B9})$$

$$F_n = 2\hbar k(A_n^* a_n + A_n a_n^\dagger). \quad (\text{B10})$$

For the beam splitter we can use following relations [similar to (A9,A26)]:

$$A_e = -\frac{A_w + A_s}{\sqrt{2}}, \quad A_n = -\frac{A_w - A_s}{\sqrt{2}}, \quad (\text{B11})$$

$$a_e = -\frac{a_w + a_s}{\sqrt{2}}, \quad a_n = -\frac{a_w - a_s}{\sqrt{2}}. \quad (\text{B12})$$

And we can write

$$F_- = \frac{F_e - F_n}{2} = \hbar k(A_w^* a_s + A_s^* a_w + A_w a_s^\dagger + A_s a_w^\dagger). \quad (\text{B13})$$

The equation of motion for the antisymmetric mode can be expressed in the next form:

$$\hbar k(A_w^* a_s + A_s^* a_w + A_w a_s^\dagger + A_s a_w^\dagger) + \mu\Omega^2 z_-(\Omega) = 0. \quad (\text{B14})$$

This equation is equivalent to (A42) with corresponding substitutions mentioned above.

2. Michelson-Sagnac interferometer

Let us now consider the Michelson-Sagnac interferometer with power and signal recycling mirrors as presented in a Fig. 2. Similarly, one can obtain a set of equations for small amplitudes in the long-wave approximation,

$$[\Gamma_w - i\Omega]a_w - i d a_s = g_w, \quad (\text{B15a})$$

$$-i d^* a_w + [\Gamma_s - i\Omega]a_s = g_s, \quad (\text{B15b})$$

where

$$\Gamma_w = \frac{1 - r_w(iT_z + \tilde{R}_+ R_z)}{r_w \tau' (iT_z + R_z)} \simeq \frac{1 - \tilde{r}_w}{\tilde{r}_w \tau'}, \quad (\text{B16})$$

$$\tilde{r}_w \equiv r_w(R_z + iT_z), \quad \tilde{R}_+ = \cos \delta\tau' \rightarrow 1, \quad (\text{B17})$$

$$\Gamma_s = \frac{1 - r_s(-iT_z + \tilde{R}_+ R_z)}{r_s \tau' (-iT_z + R_z)} \simeq \frac{1 - \tilde{r}_s}{\tilde{r}_s \tau'}, \quad (\text{B18})$$

$$\tilde{r}_s \equiv r_s(R_z - iT_z), \quad (\text{B19})$$

$$d \equiv \frac{\delta R_z}{iT_z + R_z}, \quad g_w = \frac{iT_w a_p + r_w i k X_w}{\tau' r_w (R_z + iT_z)}, \quad (\text{B20})$$

$$g_s = \frac{iT_s a_d + r_s i k X_s}{\tau' r_s (R_z - iT_z)}. \quad (\text{B21})$$

In (B20), (B21) values $X_{w,s}$ describe the influence of displacement x of the membrane,

$$X_w = 2A_s R_z x, \quad (\text{B22a})$$

$$X_s = 2A_w R_z x. \quad (\text{B22b})$$

We introduced $\tau' = \frac{2(L+l)}{c}$. Here L is the distance between the beam splitter and east (or north) mirror, l is the distance between the east (or north) mirror and the membrane, R_z is the amplitude reflectivity of the membrane, and $T_z = \sqrt{1 - R_z^2}$ is the amplitude transparency.

Formally, γ_w, γ_s are complex values; however, their imaginary parts are much smaller than the real ones due to the condition $\delta\tau' \ll 1$. In the long-wave approximations, we may put $\tilde{R}_+ \approx 1$.

Now we have to write equations for the ponderomotive forces acting on the membrane,

$$F_a = \hbar k (A_e^* a_e + A_e a_e^\dagger - A_n^* a_n - A_n a_n^\dagger), \quad (\text{B23})$$

$$F_b = \hbar k (B_e^* b_e + B_e b_e^\dagger - B_n^* b_n - B_n b_n^\dagger). \quad (\text{B24})$$

Using the following expressions in the long-wavelength approximation.

$$b_w = a_w [iT_z + R_z] + A_s R_z i 2kx, \quad (\text{B25})$$

$$b_s = a_s [-iT_z + R_z] + A_w R_z i 2kx, \quad (\text{B26})$$

$$B_w = A_w [iT_z + R_z], \quad (\text{B27})$$

$$B_s = A_s [-iT_z + R_z], \quad (\text{B28})$$

and relations for the beam splitter similar to (A9, A26),

$$A_e = -\frac{A_w + A_s}{\sqrt{2}}, \quad A_n = -\frac{A_w - A_s}{\sqrt{2}}, \quad (\text{B29a})$$

$$a_e = -\frac{a_w + a_s}{\sqrt{2}}, \quad a_n = -\frac{a_w - a_s}{\sqrt{2}}, \quad (\text{B29b})$$

$$B_e = -\frac{B_w + B_s}{\sqrt{2}}, \quad B_n = -\frac{B_w - B_s}{\sqrt{2}}, \quad (\text{B29c})$$

$$b_e = -\frac{b_w + b_s}{\sqrt{2}}, \quad b_n = -\frac{b_w - b_s}{\sqrt{2}}, \quad (\text{B29d})$$

we can rewrite equations (B23) and (B24) in the following form:

$$F_a = \hbar k (A_w^* a_s + A_w a_s^\dagger + A_s^* a_w + A_s a_w^\dagger), \quad (\text{B30})$$

$$\begin{aligned} F_b &= \hbar k (B_w^* b_s + B_w b_s^\dagger + B_s^* b_w + B_s b_w^\dagger) \\ &= \hbar k (A_w^* a_s [-iT_z + R_z]^2 + A_w a_s^\dagger [iT_z + R_z]^2 \\ &\quad + A_s^* a_w [iT_z + R_z]^2 + A_s a_w^\dagger [-iT_z + R_z]^2). \end{aligned} \quad (\text{B31})$$

And the total force acting on the membrane can be expressed by

$$\begin{aligned} F &\equiv F_a + F_b \\ &= 2\hbar k R_z (A_w^* a_s [-iT_z + R_z] + A_w a_s^\dagger [iT_z + R_z] \\ &\quad + A_s^* a_w [iT_z + R_z] + A_s a_w^\dagger [-iT_z + R_z]). \end{aligned} \quad (\text{B32})$$

Now we can write down the equation of motion for the membrane:

$$F + m\Omega^2 x(\Omega) = 0. \quad (\text{B33})$$

So we may state that formulas (B15) for the Michelson-Sagnac interferometer (MSI) are equivalent to formulas (B5) for the antisymmetric mode of the Michelson interferometer (DMMI):

- (i) Formulas for MSI transform for DMMI in limit $R_z \rightarrow 1$.
- (ii) Formulas for DMMI transform into formulas for MSI with the following substitutions in definitions of $\gamma_{w,s}$ and effective detuning d ,

$$r_{w,s} \rightarrow r_{w,s}(R_z - iT_z), \quad \tilde{R}_+ \rightarrow 1, \quad (\text{B34})$$

$$\delta \rightarrow d \equiv \alpha\delta, \quad \alpha \equiv \frac{R_z}{iT_z + R_z}. \quad (\text{B35})$$

- (iii) Formulas for DMMI transform into formulas for MSI with substitutions in definitions of right parts $g_{w,s}$ according to (B20), (B21), and (B3).

- [1] B. P. Abbott, R. Abbott, R. Adhikari, P. Ajith, B. Allen, G. Allen, R. S. Amin, S. B. Anderson, W. G. Anderson, M. A. Arain *et al.*, *Rep. Prog. Phys.* **72**, 076901 (2009).
- [2] G. M. Harry (the LIGO Scientific Collaboration), *Classical Quantum Gravity* **27**, 084006 (2010).
- [3] T. Accadia, F. Acernese, M. Alshourbagy, P. Amico, F. Antonucci, S. Aoudia, N. Arnaud, C. Arnault, K. G. Arun, P. Astone *et al.*, *JINST* **7**, P03012 (2012).
- [4] H. Grote, *Classical Quantum Gravity* **27**, 084003 (2010).
- [5] The Virgo Collaboration, Advanced Virgo Baseline Design, Report No. VIR027A09, 2009.
- [6] M. Punturo, M. Abernathy, F. Acernese, B. Allen, N. Andersson, K. Arun, F. Barone, B. Barr, M. Barsuglia, M. Beker *et al.*, *Classical Quantum Gravity* **27**, 084007 (2010).
- [7] S. Hild, M. Abernathy, F. Acernese, P. Amaro-Seoane, N. Andersson, K. Arun, F. Barone, B. Barr, M. Barsuglia, M. Beker *et al.*, *Classical Quantum Gravity* **28**, 094013 (2011).
- [8] B. Willke *et al.*, *Classical Quantum Gravity* **23**, S207 (2006).
- [9] K. Somiya, *Classical Quantum Gravity* **29**, 124007 (2012).
- [10] V. B. Braginsky, *Sov. Phys. JETP* **26**, 831 (1968).
- [11] V. B. Braginsky and Yu. I. Vorontsov, *Sov. Phys. Usp.* **17**, 644 (1975).
- [12] V. B. Braginsky, Yu. I. Vorontsov, and F. Ya. Khalili, *Sov. Phys. JETP* **46**, 705 (1977).
- [13] V. B. Braginsky and F. Ya. Khalili, *Quantum Measurement* (Cambridge University Press, Cambridge, England, 1992).
- [14] V. B. Braginsky and I. I. Minakova, *Vestnik Moskovskogo Universiteta, Fizika i Astronomiya* **1**, 83 (1967).
- [15] V. Braginsky and A. Manukin, *Sov. Phys. JETP* **25**, 653 (1967).
- [16] V. B. Braginskii, Physical experiments with test bodies (National Aeronautics and Space Administration, NASA technical translation: F-672, 1972).
- [17] V. Braginsky and F. Khalili, *Phys. Lett. A* **257**, 241 (1999).
- [18] F. Ya. Khalili, *Phys. Lett. A* **288**, 251 (2001).
- [19] A. Buonanno and Y. Chen, *Phys. Rev. D* **64**, 042006 (2001).
- [20] A. Buonanno and Y. Chen, *Phys. Rev. D* **65**, 042001 (2002).
- [21] V. I. Lazebny and S. P. Vyatchanin, *Phys. Lett. A* **344**, 7 (2005).
- [22] F. Ya. Khalili, V. I. Lazebny, and S. P. Vyatchanin, *Phys. Rev. D* **73**, 062002 (2006).
- [23] A. Nishizawa, M. Sakagami, and S. Kawamura, *Phys. Rev. D* **76**, 042002 (2007).
- [24] M. Rakhmanov, Ph.D. thesis, California Institute of Technology, 2000.
- [25] A. A. Rakhubovsky and S. P. Vyatchanin, *Phys. Lett. A* **376**, 1405 (2012).
- [26] A. Buonanno and Y. Chen, *Phys. Rev. D* **67**, 062002 (2003).
- [27] H. Rehbein, H. Müller-Ebhardt, K. Somiya, S. L. Danilishin, C. Li, R. Schnabel, K. Danzmann, and Y. Chen, *Phys. Rev. D* **78**, 062003 (2008).
- [28] A. A. Rakhubovsky, S. Hild, and S. P. Vyatchanin, *Phys. Rev. D* **84** (2011).
- [29] T. Corbitt, Y. Chen, E. Innerhofer, H. Müller-Ebhardt, D. Ottaway, H. Rehbein, D. Sigg, S. Whitcomb, C. Wipf, and N. Mavalvala, *Phys. Rev. Lett.* **98**, 150802 (2007).
- [30] S. P. Tarabrin, H. Kaufer, F. Ya. Khalili, R. Schnabel, and K. Hammerer, *Phys. Rev. A* **88**, 023809 (2013).
- [31] D. Friedrich, H. Kaufer, T. Westphal, K. Yamamoto, A. Sawadsky, F. Khalili, S. Danilishin, S. Gothler, K. Danzmann, and R. Schnabel, *New J. Phys.* **13**, 093017 (2011).
- [32] K. Yamamoto, D. Friedrich, T. Westphal, S. Goßßler, K. Danzmann, K. Somiya, S. Danilishin, and R. Schnabel, *Phys. Rev. A* **81**, 033849 (2010).
- [33] A. Xuereb, R. Schnabel, and K. Hammerer, *Phys. Rev. Lett.* **107**, 213604 (2011).
- [34] F. Khalili, S. Danilishin, H. Miao, H. Müller-Ebhardt, H. Yang, and Y. Chen, *Phys. Rev. Lett.* **105**, 1 (2010).
- [35] J. D. Thompson, B. M. Zwickl, A. M. Jayich, F. Marquardt, S. M. Girvin, and J. G. E. Harris, *Nature (London)* **452**, 72 (2008).
- [36] E. Verhagen, S. Weis, A. Schliesser, and T. J. Kippenberg, *Nature (London)* **482**, 63 (2012).
- [37] M. Eichenfield, J. Chan, R. M. Camacho, K. J. Vahala, and O. Painter, *Nature (London)* **462**, 78 (2009).
- [38] M. R. Vanner, I. Pikovski, G. D. Cole, M. S. Kim, C. Bukner, K. Hammerer, G. J. Milburn, and M. Aspelmeyer, *Proc. Natl. Acad. Sci. U.S.A.* **108**, 16182 (2011).
- [39] S. Danilishin and F. Y. Khalili, *Living Rev. Relativity* **15**, 5 (2012).
- [40] S. P. Vyatchanin, *Sov. Phys. Dokl.* **23**, 321 (1977).
- [41] F. Marquardt, A. A. Clerk, and S. M. Girvin, *J. Mod. Opt.* **55**, 3329 (2008).
- [42] Advanced LIGO reference design, 2005, http://www.ligo.caltech.edu/advLIGO/scripts/ref_des.shtml.
- [43] H. Kimble, Yu. Levin, A. Matsko, K. Thorne, and S. Vyatchanin, *Phys. Rev. D* **65**, 022002 (2001).